

ApJ

DISCOVERY OF A NEW DUSTY B[E] STAR IN THE SMALL MAGELLANIC CLOUD

JOHN P. WISNIEWSKI^{1,2,3}, KAREN S. BJORKMAN^{3,4}, JON E. BJORKMAN⁴, MARK CLAMPIN²
Draft version July 6, 2007

ABSTRACT

We present new optical spectroscopic and Spitzer IRAC photometric observations of a B-type star in the SMC cluster NGC 346, NGC 346:KWBBE 200. We detect numerous Fe II, [O I], [Fe II], as well as strong P-Cygni profile H I emission lines in its optical spectrum. The star's near-IR color and optical to IR SED clearly indicate the presence of an infrared excess, consistent with the presence of gas and warm, $T \sim 800$ K, circumstellar dust. Based on a crude estimate of the star's luminosity and the observed spectroscopic line profile morphologies, we find that the star is likely to be a B-type supergiant. We suggest that NGC 346:KWBBE 200 is a newly discovered B[e] supergiant star, and represents the fifth such object to be identified in the SMC.

Subject headings: circumstellar matter — Magellanic Clouds — stars: individual (NGC346:KWBBE 200) — stars: individual ([MA93] 1116 — stars: emission-line, Be

1. INTRODUCTION

Massive OB stars play an important role in astrophysics; their winds and ejecta shape the morphology and ionization structure of their local environment, and provide a source of heavy elements which serve as the building blocks of planetary systems. B[e] stars comprise a heterogeneous group of massive stars which all exhibit similar observational properties, yet range in evolutionary age from the pre- to post-main sequence (Lamers et al. 1998). B[e] supergiants (B[e]SGs) represent one sub-class of the B[e] phenomenon and are notable in that at least some share similar photometric, spectroscopic, and rotational velocity properties as Luminous Blue Variables (LBVs) (Stahl et al. 1983; Zickgraf et al. 1996; van Genderen & Sterken 2002; Zickgraf 2006), which suggests B[e]SGs might be precursors to LBVs.

B-type stars which exhibit strong H I Balmer emission, forbidden and low excitation emission lines, commonly Fe II, [Fe II], and [O I], and evidence of warm ($T \sim 1000$ K) dust are assigned the classification of B[e] (Allen & Swings 1976; Lamers et al. 1998; Zickgraf 2006). B[e]SGs are known to exhibit a hybrid spectrum characterized by broad UV resonance absorption lines and a wealth of narrow emission lines (Zickgraf et al. 1985, 1986). Zickgraf et al. (1985) suggested that a non-spherical wind model consisting of a cool, equatorial component, and a hot, polar component best explained these observations. Subsequent polarimetric observations seem to confirm the presence of an axisymmetric circumstellar environment in B[e]SGs (Magalhães 1992; Schulte-Ladbeck & Clayton 1993; Melgarejo et al. 2001), the base of which may sometimes be clumpy (Magalhães et al. 2006). While polarimetric observations of LBVs and LBV-like objects (Taylor et al. 1991; Nordsieck et al. 2001; Davies et al. 2005; Wisniewski et al. 2007) indicate the presence of an asymmetric, clumpy wind, it is not yet clear whether they exhibit a clumpy,

axi-symmetric geometry similar to that observed for B[e] stars (see e.g. Davies et al. 2005), which might be expected if B[e]SGs are truly precursors of LBVs.

To date, four B[e] stars have been identified in the Small Magellanic Cloud (SMC) while eleven have been identified in the Large Magellanic Cloud (LMC). Owing to the known distance of the SMC and LMC and the observed luminosities of the fifteen SMC and LMC B[e] sources, it is well accepted that all are B[e]SGs (Zickgraf 2006). In this paper, we report the serendipitous discovery of the fifth known B[e] star in the SMC. The star was initially classified by Meyssonier & Azzopardi (1993) as a compact H II source ([MA93] 1116) likely characterized by broad H α emission. A later optical photometric survey by Keller et al. (1999) classified the same target (NGC346:KWBBE 200) as a classical Be star residing in the SMC cluster NGC 346, which is known to be a rich source of current and recent star formation (Nota et al. 2006; Sabbi et al. 2007). Our observations of the source were obtained in the context of assessing the formation and evolution of classical Be stars in NGC 346 and other clusters in the SMC and LMC (Wisniewski & Bjorkman 2006; Wisniewski et al. 2007).

2. OBSERVATIONS

Our spectroscopic observations were obtained on 15 November 2004 using the Cerro Tololo Inter-American Observatory (CTIO) 4m telescope Hydra 138 fiber multi-object spectrograph. We used the 527 lines mm^{-1} KPGL3 grating and a 200 μm slit plate, yielding a dispersion of 1.75 \AA at 5500 \AA ($R \sim 3000$). We obtained two 3600 second exposures with NGC 346:KWBBE 200 in a fiber; for each exposure, we also assigned fourteen fibers to locations void of stellar sources to serve as probes of background sky emission. Our NGC 346 exposures were bracketed by observations of a penray lamp exposure to wavelength calibrate our data. Standard bias frames and dome flats

¹ NPP Fellow

² NASA GSFC Exoplanets and Stellar Astrophysics Lab Code 667, Greenbelt, MD 20771, John.P.Wisniewski@nasa.gov, Mark.Clampin@nasa.gov

³ Visiting Astronomer, Cerro Tololo Inter-American Observatory

⁴ Ritter Observatory, MS #113, Department of Physics and Astronomy, University of Toledo, Toledo, OH 43606, Karen.Bjorkman@utoledo.edu, Jon.Bjorkman@utoledo.edu

were obtained at the beginning of each night of our run; sky flats were also obtained to calibrate the fiber-to-fiber throughput of Hydra.

Following bias subtraction using standard IRAF techniques, we used Pieter van Dokkum’s *L.A. Cosmic* routine to identify and remove cosmic ray artifacts from our images. Remaining standard reduction steps, including flat fielding, aperture extraction, and wavelength calibration were done within the *Hydra* IRAF package. To subtract the strong nebular lines present in our data, we evaluated the use of various combinations of our fourteen sky fibers in an iterative manner. Following our best subtraction, we only see evidence of residual nebular contamination from [O III] lines at 4959 and 5007 Å, at an intensity of 2% of the total sky emission in these transitions. We do not observe other narrow (GFWHM ~ 2.9 Å) emission profiles at other wavelengths, which would be indicative of a nebular origin; hence, we estimate that any residual nebular components still present in our data should contribute $< 2\%$ to the equivalent widths quoted in this paper.

We also present archival *Spitzer Space Telescope* Infrared Array Camera (IRAC; Fazio et al. 2004) 3.6, 4.5, 5.8, and 8 μm observations of NGC 346:KWBBE 200, obtained as part of program 63 (Houck PI). The data were reduced via the *Spitzer* pipeline S14.0 software. Photometry was extracted from post-pipeline mosaic images using standard IRAF *DAOPHOT* aperture photometry techniques; uncertainties in the absolute flux calibration are less than 5% (Laine & Reach 2006).

3. RESULTS

3.1. Optical Spectroscopy

The continuum normalized optical spectrum of NGC 346:KWBBE 200 from 3935–5365 Å and 6000–6540 Å is presented in Figures 1 and 2 respectively. Continuum signal to noise levels range from ~ 20 at 4200 Å to ~ 70 at 5200 and 6200 Å. NGC 346:KWBBE 200 is clearly characterized by a wealth of emission lines; we used line identifications reported by Zickgraf et al. (1989); Gummertsbach et al. (1995); de Winter & van den Ancker (1997); Lamers et al. (1998) and Miroschnichenko et al. (2005) to identify the strongest lines detected at the resolution of our data, which are labeled in the figures and tabulated in Table 1. The dominant species seen in emission is Fe II, although lines of [Fe II], [O I], Mg I, and Ti II also are present.

NGC 346:KWBBE 200 is also characterized by strong H I emission, from H ϵ (Figure 1) through H α (Figure 3), with all lines clearly exhibiting P-Cygni profiles indicative of a strong outflowing wind. The H α line is particularly strong and broad; we measured our second exposure to have a net equivalent width of ~ -267 Å and wings extending to -2100 km s $^{-1}$ and $+2190$ km s $^{-1}$. Similarly, we measured H α in our first exposure to have a net equivalent width of -266 Å and wings extending to -2100 km s $^{-1}$ and $+2100$ km s $^{-1}$. The dominant source of uncertainty in these measurements is not photon statistics, but rather given the presence of extended electron scattering wings and the curvature of the spectral response of the grating+detector near H α , our choice of continuum placement. Spectra of emission- and non-emission line stars located in other Hydra fibers were used to calibrate the typical spectral response behavior near H α , providing a constraint on the appropriate

order of fitting function to use to fit the continuum region near H α for NGC 346:KWBBE 200.

3.2. Optical and IR Photometry

To further explore the nature of NGC 346:KWBBE 200, we plot the star on a near-IR 2-color diagram (black star; Figure 4), along with likely Magellanic Cloud classical Be stars from de Wit et al. (2005) (red triangles) and Wisniewski et al. (2007) (green triangles), a potential LMC Herbig Ae/Be star (blue cross) from de Wit et al. (2005), and known SMC and LMC B[e]SGs (blue circles) from McGregor et al. (1988), Gummertsbach et al. (1995), and the 2MASS catalog. NGC 346:KWBBE 200’s near-IR color is clearly consistent with that observed for other SMC/LMC B-type stars characterized by dusty circumstellar envelopes, and is inconsistent with the typical color of classical Be stars, which are characterized by gaseous circumstellar disks (Porter & Rivinius 2003).

We next construct NGC 346:KWBBE 200’s spectral energy distribution (SED), using all available photometry. Its observed (B-V) and (V-I) colors, 0.351 and 0.366 (Zaritsky et al. 2002), are substantially redder than the expected intrinsic colors of main sequence ($-0.30 < (B-V)_o < -0.07$, Schmidt-Kaler 1982; $-0.44 < (V-I)_o < -0.11$, Ducati et al. 2001) or supergiant-type ($-0.23 < (B-V)_o < 0.0$, Schmidt-Kaler 1982; $-0.37 < (V-I)_o < 0.0$, Ducati et al. 2001) B stars. As such, we have assumed that NGC 346:KWBBE 200 is characterized by a *minimum* E(B-V) reddening of 0.35, and de-reddened its U- through K-band photometry using $R_V = 2.74$ (Gordon et al. 2003) and the standard extinction curves of Cardelli et al. (1989). The resultant SED incorporating U-band through *Spitzer* IRAC 8 μm photometry is shown in Figure 5. An excess of IR emission is evident both at near-IR (J-band) wavelengths, likely originating from free-free and bound-free emission from hydrogen in a circumstellar envelope (or disk), and at IRAC-band IR wavelengths, indicating the presence of warm dust in a circumstellar envelope (or disk) (see e.g. Zickgraf et al. 1985, 1989). To crudely characterize this dust component, we have overlaid a Planck function corresponding to a dust temperature of $T = 800\text{K}$ in Figure 5, which we believe best represents the observed SED trend.

4. DISCUSSION

4.1. NGC 346:KWBBE 200’s Status as a B[e] Star

We have shown that NGC 346:KWBBE 200’s optical spectrum is dominated by emission lines from Fe II, [O I], and [Fe II]. It exhibits broad P-Cygni profile H I emission lines, indicative of a strong outflowing wind; the strength of its H α equivalent width, ~ -267 Å is rivaled only by other known B[e]SGs (Zickgraf et al. 1989) and some LBVs (Davies et al. 2005). The star’s circumstellar environment is clearly characterized by the presence of both gas and warm dust, as diagnosed from its near-IR colors (Figure 4) and near- and IR-SED excess (Figure 5). These observational properties are characteristic of B[e] stars (Allen & Swings 1976; Lamers et al. 1998; Zickgraf 2006), and inconsistent with the expected behavior of classical Be stars; thus, we suggest that NGC 346:KWBBE 200 should be reclassified as the fifth known B[e] star in the SMC.

4.2. Evolutionary Status

To constrain the evolutionary status of NGC 346:KWBBE 200, we compared its de-reddened photometry to standard Kurucz model atmospheres (Kurucz 1992) using $\log(Z/Z_{sun}) = -1.0$ and $\log(g) = 3.5$. As shown in Figure 5 and summarized in Table 2, the SED data are best represented by a model having $T_{eff} = 19,000$ K, and $R_{star} = 14 R_{sun}$ (Figure 5). Given the significant uncertainty over the exact E(B-V) reddening associated with NGC 346:KWBBE 200, we caution that these stellar parameters should only be considered initial estimates; the presence of a higher E(B-V) reddening than assumed here (0.35) will inflate T_{eff} and modify R_{star} . Nonetheless, assuming a standard relationship that $L_{star} = (R_{star}/R_{sun})^2 (T_{eff}/T_{sun})^4$, we can estimate the luminosity of NGC 346:KWBBE 200 to be $\log(L/L_{sun}) \sim 4.4$ (Table 2). These stellar parameters correspond to crude spectral classification of B3[e] II.

Using these crude stellar parameters, we plot NGC 346:KWBBE 200 on a Hertzsprung-Russell (HR) diagram (black circle), along with other known SMC, LMC, and Galactic B[e]SG (green, red, and blue triangles) and pre-main sequence Herbig B[e] (hereafter HAeB[e]) stars (yellow squares) in Figure 6. The canonical (non-accreting) evolutionary tracks (Bernasconi 1996) and zero-age main sequence (ZAMS) for 9 and 15 M_{sun} stars at a metallicity appropriate for the SMC/LMC, $z = 0.001$ (black lines), and for 3 and 5 M_{sun} stars at a metallicity appropriate for the Galactic HAeBe stars, $z = 0.020$ (red lines), are also plotted in Figure 6, along with the birthline for the $z = 0.020$ models (solid light blue line) and isochrones for the $z = 0.001$ models (dashed green, blue, and yellow lines). It is clear that NGC 346:KWBBE 200 is well above the birthline of late-type B stars (5 M_{sun}) and is most similar to the lower luminosity Magellanic Cloud B[e]SGs stars reported by Gummertsbach et al. (1995). If it were a pre-MS star, inspection of Figure 6 indicates the star would be positioned at a youthful position along the the $z = 0.001$ 15 M_{sun} evolutionary track, and intersect the $\log(T) = 4.25$ isochrone. Such a young, high-mass object would likely still be deeply embedded in its natal star formation envelope, in contradiction to the star's observed optical v-band magnitude and our easily detection of its optical spectrum.

Lamers et al. (1998) provided a nice discussion of the classification of B[e] stars and established numerous criteria for determining whether a B[e] star is a B[e]SG, HAeB[e], compact planetary nebula B[e], Symbiotic B[e], or an "unclassified" B[e] star, which we briefly review here. To be considered a B[e]SG, Lamers et al. (1998) suggest stars should obey two primary criteria: A1) exhibit the B[e] phenomenon; and A2) be supergiants with $\log(L/L_{sun}) \geq 4.0$; and four secondary criteria, two of which are: B1) optical spectroscopic evidence of mass loss; and B2) typically exhibit small photometric variations of order 0.1^m . To be considered a HAeB[e], Lamers et al. (1998) suggest stars should obey three primary criteria: A1) exhibit the B[e] phenomenon; A2) be associated with a star forming region; and A3) exhibit evidence of accretion via inverse P Cygni spectroscopic line profiles; and three secondary criteria: B1) exhibit a luminosity of $\log(L/L_{sun}) \leq 4.5$; B2) exhibit large, irregular photometric variations; and B3) exhibit evidence of warm and cool dust

in their SEDs. Note that some of the criteria for B[e]SG and HAeB[e] designations overlap; moreover, a growing body of evidence suggests that some B[e]SGs may also exhibit significant, large amplitude photometric variability (Zickgraf et al. 1996; van Genderen & Sterken 2002), indicating that this behavior is not exclusive to HAeB[e] stars.

NGC 346:KWBBE 200's strong P-Cygni profile H I emission is indicative of mass-loss; we observe no evidence of inverse P-Cygni profiles which would be indicative of infall. As shown in Figure 6, NGC 346:KWBBE 200's crudely derived luminosity, $\log(L/L_{sun}) \sim 4.4$, and location on a HR diagram is more consistent with the star being a low luminosity B[e]SG than a high luminosity HAeB[e] star. The star does reside in a young cluster, portions of which are actively forming low-mass stars (Nota et al. 2006; Sabbi et al. 2007), which seemingly agrees with the aforementioned "A2" criteria of HAeB[e] stars; however, other well known highly evolved massive stars reside in the region (e.g. the Wolf-Rayet/LBV HD 5980; aka NGC 346:KWBBE 200 ?) hence this particular criteria is probably not a useful discriminant in this situation. As such, given the available data presently available for NGC 346:KWBBE 200, we suggest the star is a B[e]SG, similar to the other 4 known SMC and 11 LMC B[e] identified to date (Gummertsbach et al. 1995; Lamers et al. 1998).

5. SUMMARY AND FUTURE WORK

NGC 346:KWBBE 200 is a B-type star whose optical spectrum is dominated by Fe II, [O I], [Fe II], and strong P-Cygni H I emission lines, and exhibits clear evidence of having a circumstellar envelope characterized by the presence of gas and warm ($T_{duct} \sim 800$ K) dust. Based on these observational properties, we suggest that NGC 346:KWBBE 200 is a B[e]SG star, representing the fifth such object identified to date in the SMC. Our crude estimate of the star's luminosity, $\log(L/L_{sun}) \sim 4.4$, its location on a HR diagram, and its observed line profile morphologies suggests it is most likely to be a B[e] supergiant.

We recommend several observational approaches be pursued to further constrain the evolutionary status of NGC 346:KWBBE 200. Mid- to far-IR photometric observations would allow one to search for the presence of cool dust, which is one of the defining characteristics of HAeB[e] stars (Lamers et al. 1998) and would not be an expected characteristic of B[e]SGs. Moreover, high resolution optical and UV spectroscopic observations would facilitate a more reliable estimate of NGC 346:KWBBE 200's spectral type and luminosity to be derived, hence provide more conclusive evidence of the post-main sequence evolutionary status suggested in this paper. Optical photometric monitoring, to search for and characterize variability, and measurements of the star's rotational velocity would aid efforts to explore evolutionary links between the B[e]SG and LBV phases of massive star evolution.

We thank Ted Gull and Aki Roberge for helpful discussions about these results. We also thank the anonymous referee for providing useful feedback which improved the content and presentation of this paper. Support for this project was provided by NASA NPP and GSRP fellowships to JPW (NNH06CC03B, NGT5-50469), a NASA LTSA grant NAG5-8054 and a Research Corporation Cot-

trell Scholar award to KSB, and a NSF grant (AST-0307686) to JEB. This work is based in part on observations made with the Spitzer Space Telescope, which is operated by the Jet Propulsion Laboratory, California In-

stitute of Technology under a contract with NASA. We have also made use of the SIMBAD database operated at CDS, Strasbourg, France, and the NASA ADS system.

REFERENCES

- Allen, D.A. & Swings, J.P. 1976, *A&A*, 47, 293
Bernasconi, P.A. 1996, *A&AS*, 120, 57
Cardelli, J.A., Clayton, G.C., & Mathis, J.S. 1989, *ApJ*, 345, 245
Davidson, K. et al. 2005, *AJ*, 129, 900
Davies, B., Oudmaijer, R.D., & Vink, J.S. 2005, *A&A*, 439, 1107
de Winter, D. & van den Ancker, M.E. 1997, *A&AS*, 121, 275
de Wit, W.J., Beaulieu, J.-P., Lamers, H.J.G.L.M., Coutures, C., & Meeus, G. 2005, *A&A*, 432, 619
Ducati, J.R., Bevilacqua, C.M., Rembold, S.B., & Ribeiro, D. 2001, *ApJ*, 558, 309
Fazio, G.G. et al. 2004, *ApJS*, 154, 10
Gordon, K.D., Clayton, G.C., Misselt, K.A., Landolt, A.U., & Wolff, M.J. 2003, *ApJ*, 594, 279
Gummersbach, C.A., Zickgraf, F.-J., & Wolf, B. 1995, *A&A*, 302, 409
Henning, Th., Burkert, A., Launhardt, R., Leinert, Ch., & Stecklum, B. 1998, *A&A*, 336, 565
Keller, S.C., Wood, P.R., & Bessell, M.S. 1999, *A&AS*, 134, 489
Kurucz, R.L. 1992, in *IAU Symp. 149, The Stellar Populations of Galaxies*, ed. B. Barbuy & A. Renzini (Dordrecht: Kluwer), 225
IRAC Data Handbook v3.0 (ed. S. Laine & B. Reach), 2006, v3.0
Lamers, J.G.L.M., Zickgraf, F.-J., de Winter, D., Houziaux, & Zorec, J. 1998, *A&A*, 340, 117
Magalhães, A.M. 1992, *ApJ*, 398, 286
Magalhães, A.M., Melgarejo, R., Pereyra, A., & Carciofi, A.C. 2006, in *Stars with the B[e] Phenomenon*, ed. M. Kraus & A. Miroshnichenko, *ASP Conf. Proc.* 355, 147
McGregor, P.J., Hillier, D.J., & Hyland, A.R. 1988, *ApJ*, 334, 639
Melgarejo, R., Magalhães, A.M., Carciofi, A.C., & Rodrigues, C.V. 2001, *A&A*, 377, 581
Meyssonnier, N. & Azzopardi, M. 1993, *A&AS*, 102, 451
Miroshnichenko, A.S., Bjorkman, K.S., Grosso, M., Hinkle, K., Levato, H., & Marang, F. 2005, *A&A*, 436, 653
Nordsieck, K.H. et al. 2001, in *ASP Conf. Ser.* 233, P Cygni 2000: 400 Years of Progress, ed. M. de Groot & C. Sterken (San Francisco:ASP), 261
Nota, A. et al. 2006, *ApJL*, 640, 29
Porter, J.M. & Rivinius, T. 2003, *PASP*, 115, 1153
Sabbi, E. et al. 2007, *AJ*, 133, 44
Schmidt-Kaler, T.H. 1982, in *Landolt-Bornstein, New Series, Group VI, Vol. 2b, Stars and Star Clusters*, ed. K. Schaifers & H.H. Voigt (New York: Springer)
Schulte-Ladbeck, R.E. & Clayton, G.C. 1993, *AJ*, 106, 790
Stahl, O., Wolf, B., Zickgraf, F.-J., Bastian, U., de Groot, M.J.H., & Leitherer, C. 1983, *A&A*, 120, 287
Taylor, M., Nordsieck, K.H., Schulte-Ladbeck, R.E., & Bjorkman, K.S. 1991, *AJ*, 102, 1197
van Genderen, A.M. & Sterken, C. 2002, *A&A*, 386, 926
Vinkovic, D. & Jurkic, T. 2007, *ApJ*, 658, 462
Wisniewski, J.P. & Bjorkman, K.S. 2006, *ApJ*, 652, 458
Wisniewski, J.P., Babler, B.L., Bjorkman, K.S., Kurchakov, A.V., Meade, M.R., & Miroshnichenko, A.S. 2006, *PASP*, 118, 820
Wisniewski, J.P., Bjorkman, K.S., Magalhães, A.M., Bjorkman, J.E., Meade, M.R., & Pereyra, A. 2007, *ApJ*, submitted
Zaritsky, D., Harris, J., Thompson, I.B., Grebel, E.K., & Massey, P. 2002, *AJ*, 123, 855
Zickgraf, F.-J., Wolf, B., Stahl, O., Leitherer, C., & Klare, G. 1985, *A&A*, 143, 421
Zickgraf, F.-J., Wolf, B., Stahl, O., Leitherer, C., & Appenzeller, I. 1986, *A&A*, 163, 119
Zickgraf, F.-J., Wolf, B., Stahl, O., & Humphreys, R.M. 1989, *A&A*, 220, 206
Zickgraf, F.-J., Kovacs, J., Wolf, B., Stahl, O., Kaufer, A., & Appenzeller, I. 1996, *A&A*, 309, 505
Zickgraf, F.-J. 2006, in *Stars with the B[e] Phenomenon*, ed. M. Kraus & A. Miroshnichenko, *ASP Conf. Proc.* 355, 135

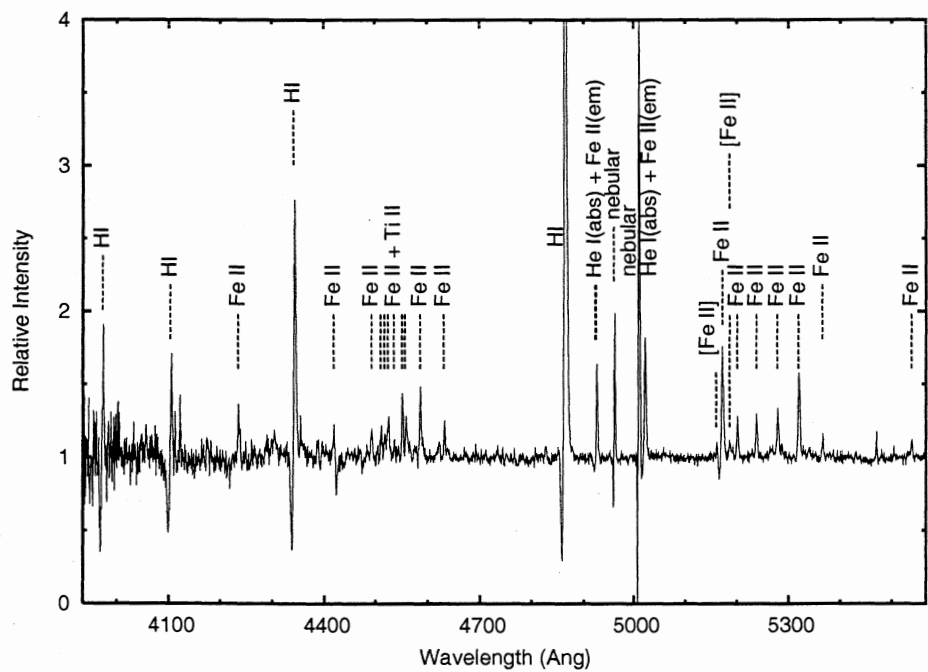


FIG. 1.— The blue portion of NGC 346:KWBe 200's optical spectrum is dominated by Fe II, [Fe II], and H I emission lines. These transitions are typically observed in B[e] stars (Allen & Swings 1976; Lamers et al. 1998; Zickgraf 2006).

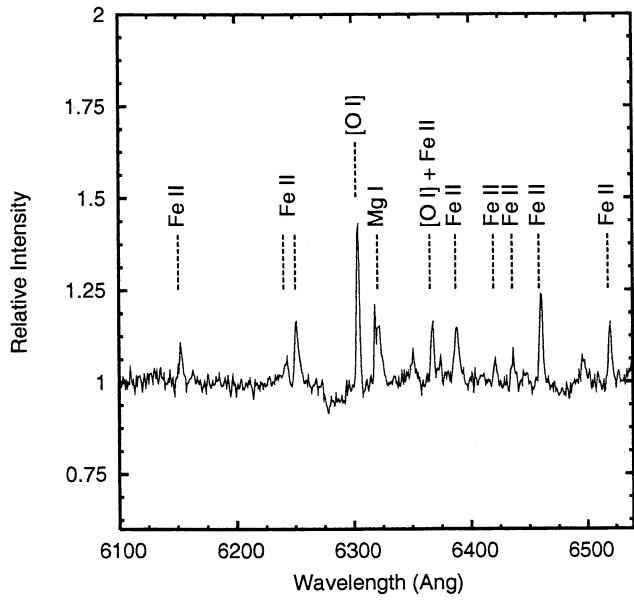


FIG. 2.— The red portion of NGC 346:KWBBe 200's optical spectrum is dominated by Fe II and [O I] emission lines, which along with the transitions observed in the blue portion of the spectrum (Figure 1), are typically observed in B[e] stars (Allen & Swings 1976; Lamers et al. 1998; Zickgraf 2006).

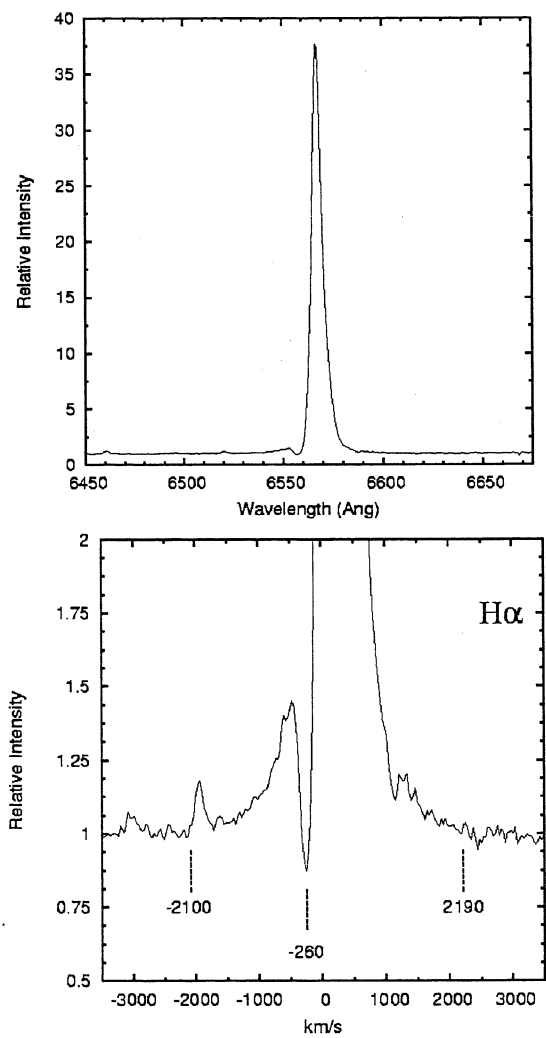


FIG. 3.— The net emission strength ($\sim -267 \text{ \AA}$), line-profile morphology (P-Cygni), and broad electron scattering wings ($\sim -2100 \text{ km s}^{-1}$ and $\sim +2190 \text{ km s}^{-1}$) of the H α line in NGC 346:KWBBE 200 is similar to that observed in other B[e]SGs (Zickgraf et al. 1989).

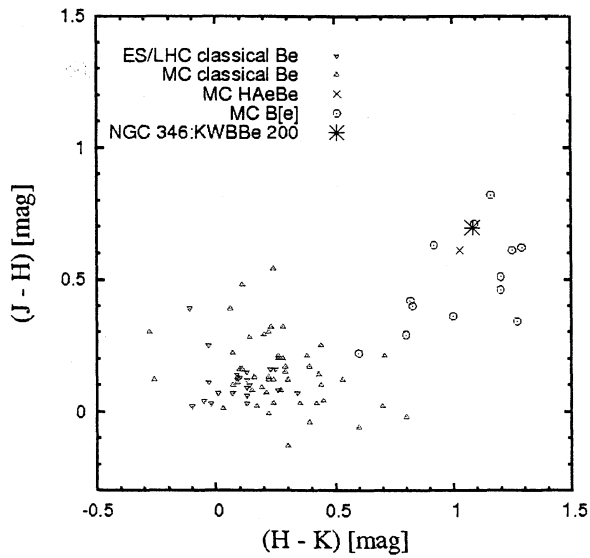


FIG. 4.— The location of NGC 346:KWBBe 200 (black star), along with likely Magellanic Cloud classical Be stars from de Wit et al. (2005) (red triangles) and Wisniewski et al. (2007) (green triangles), a potential Herbig Ae/Be star (blue cross) in the LMC (de Wit et al. 2005), and known Magellanic Cloud B[e]SGs (blue circles) from McGregor et al. (1988), Gummersbach et al. (1995), and the 2MASS catalog are shown on a near-IR 2-color diagram. NGC 346:KWBBe 200's near-IR color clearly coincides with that of other dusty Magellanic Cloud (B[e] and Herbig Ae/Be) stars and is inconsistent with the observed near-IR colors of Magellanic Cloud classical Be stars.

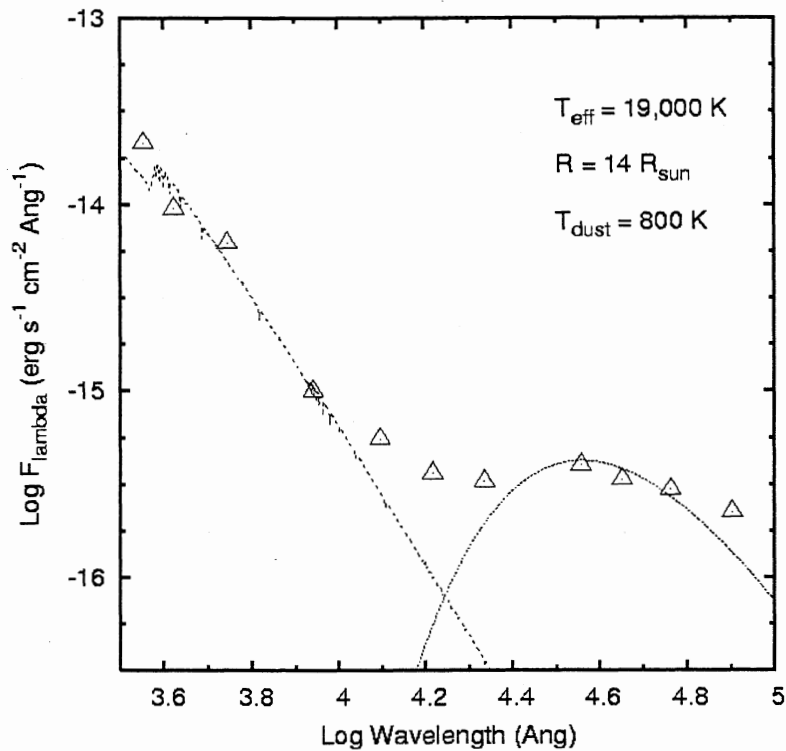


FIG. 5.— The SED of NGC 346:KWBBe 200 following dereddening of its optical and near-IR (J,H,K) photometry, assuming $E(B-V) = 0.35$. An excess of infrared flux is clearly present, indicating the presence of gas and warm, $T_{\text{dust}} \sim 800\text{K}$, dust. The optical photometry are consistent with a Kurucz model atmosphere having $T_{\text{eff}} = 19,000\text{K}$ and $R_{\text{star}} = 14 R_{\text{sun}}$. The extrapolated stellar luminosity, $\log(L/L_{\text{sun}}) \sim 4.4$, and observed line profile morphologies suggest that NGC 346:KWBBe 200 is a B[e]SG.

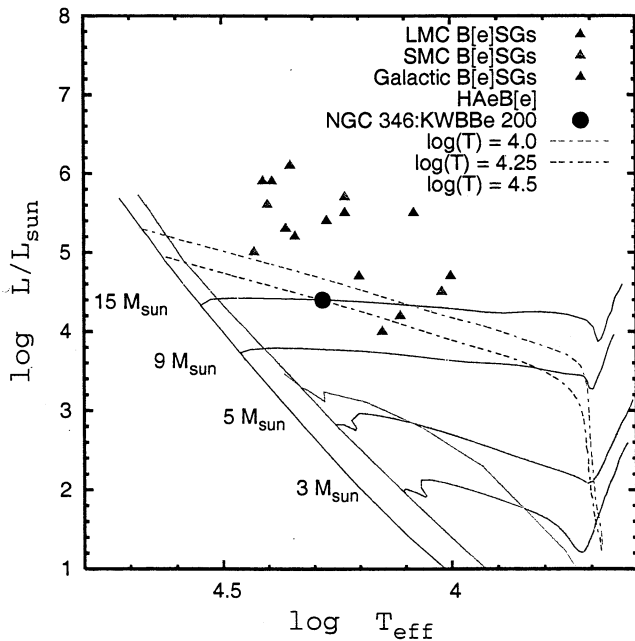


FIG. 6.— NGC 346:KWBBE 200 (black circle) plotted on a HR diagram, along with other known LMC, SMC, and Galactic B[e]SGs (red, green, and blue triangles respectively) and Galactic HAeBe stars (yellow squares). Temperature and luminosity values for these ancillary sources were from (Lamers et al. 1998) and references therein for all sources except for the luminosity of MWC 1080 (Henning et al. 1998) and V594 Cas (Vinkovic & Jurkic 2007). Also overplotted are canonical evolutionary tracks and the ZAMS for $z = 0.001$ 9 and $15 M_{\text{sun}}$ stars (black lines) and $z = 0.020$ 3 and $5 M_{\text{sun}}$ stars (red lines), the birthline for the $z = 0.020$ models (light blue line), and isochrones for the $z = 0.001$ models (dashed green, blue, and yellow lines). NGC 346:KWBBE 200 appears to be more similar to the lower luminosity Magellanic Cloud B[e]SGs stars reported by Gummertsbach et al. (1995) than to the relative position of other known HAeBe stars; furthermore, its observed photometric and spectroscopic properties do not indicate that the star is highly embedded in a natal star formation envelope, as it would be if it were truly located at the $\log(T) = 4.25$ isochrone of the $15 M_{\text{sun}}$ pre-MS evolutionary track of (Bernasconi 1996).

TABLE 1
SUMMARY OF OBSERVED EMISSION AND ABSORPTION FEATURES

| Wavelength | Line | EW (Å) | comment |
|------------|---------------|--------|----------------------|
| 3970 | H ϵ | ... | P-Cygni |
| 4101 | H δ | 0.4 | P-Cygni |
| 4233 | Fe II | -1.3 | ... |
| 4340 | H γ | -5.2 | P-Cygni |
| 4417 | Fe II | ... | ... |
| 4491 | Fe II | ... | blend ¹ |
| 4508 | Fe II | ... | ... |
| 4515 | Fe II | ... | ... |
| 4522 | Fe II | ... | blend ² |
| 4534 | Ti II + Fe II | ... | blend ³ |
| 4549 | Fe II + Ti II | ... | blend ⁴ |
| 4555 | Fe II | ... | ... |
| 4584 | Fe II | ... | ... |
| 4629 | Fe II | ... | ... |
| 4861 | H β | -29.3 | P-Cygni ⁵ |
| 4921 | He I | ... | abs |
| 4924 | Fe II | -2.3 | ... |
| 5015 | He I | ... | abs |
| 5018 | Fe II | -3.5 | ... |
| 5158 | [Fe II] | ... | ... |
| 5169 | Fe II | ... | P-Cygni? |
| 5184 | [Fe II] | ... | ... |
| 5198 | Fe II | -1.0 | ... |
| 5235 | Fe II | -1.2 | ... |
| 5276 | Fe II | ... | ... |
| 5317 | Fe II | -2.4 | ... |
| 5363 | Fe II | ... | ... |
| 5535 | Fe II | ... | ... |
| 6148 | Fe II | -0.4 | ... |
| 6238 | Fe II | ... | ... |
| 6248 | Fe II | -0.7 | ... |
| 6300 | [O I] | -1.2 | ... |
| 6318 | Mg I | ... | ... |
| 6363 | [O I] + Fe II | ... | blend ⁶ |
| 6385 | Fe II | -0.8 | ... |
| 6417 | Fe II | ... | ... |
| 6433 | Fe II | ... | ... |
| 6456 | Fe II | ... | ... |
| 6516 | Fe II | ... | ... |
| 6563 | H α | -267 | P-Cygni ⁷ |

Note. — line identifications are tabulated for the strongest lines in NGC 346:KWBe 200's optical spectrum. Net equivalent width measurements are also cited for all lines which exhibit no significant evidence of blending. ¹ blend of Fe II 4489+4491 Å; ² blend of Fe II 4520,4522 Å; ³ blend of Ti II 4533 + Fe II 4534 Å; ⁴ blend of Fe II 4549 + Ti II 4549 Å; ⁵ wings extend to -840 km s⁻¹, +1220 km s⁻¹; ⁶ blend of [O I] 6363 + Fe II 6369 Å; ⁷ EW excludes Fe II 6516Å.

TABLE 2
PHOTOMETRY AND SUMMARY OF FUNDAMENTAL PARAMETERS

| Parameter | Value |
|--|--------------------------|
| U | 14.834 ±0.048 |
| B | 15.957 ±0.048 |
| V | 15.606 ±0.038 |
| I | 15.240 ±0.148 |
| J | 14.551 ±0.046 |
| H | 13.855 ±0.043 |
| K' | 12.772 ±0.032 |
| 3.6 μm | 10.53 ±0.05 ¹ |
| 4.5 μm | 9.76 ±0.04 ¹ |
| 5.8 μm | 8.85 ±0.04 ¹ |
| 8.0 μm | 7.81 ±0.03 ¹ |
| T _{eff} | ~19000 K |
| R _{star} | ~14 R _{solar} |
| log (L _{star} /L _{solar}) | ~4.4 |
| T _{dust} | ~800 K |

Note. — The optical and near-IR photometry for NGC 346:KWBBE 200 has been extracted from the catalog of Zaritsky et al. (2002). ¹ The quoted Spitzer IRAC-band photometric errors do not include absolute calibration uncertainties, which is estimated to be <5% (Laine & Reach 2006).